

Article

Indirect effects shape species fitness in coevolved mutualistic networks

<https://doi.org/10.1038/s41586-023-06319-7>

Received: 11 January 2023

Accepted: 13 June 2023

Published online: 19 July 2023

 Check for updates

Leandro G. Cosmo¹✉, Ana Paula A. Assis², Marcus A. M. de Aguiar³, Mathias M. Pires⁴, Alfredo Valido⁵, Pedro Jordano^{6,7}, John N. Thompson⁸, Jordi Bascompte⁹ & Paulo R. Guimarães Jr¹⁰

Ecological interactions are one of the main forces that sustain Earth's biodiversity. A major challenge for studies of ecology and evolution is to determine how these interactions affect the fitness of species when we expand from studying isolated, pairwise interactions to include networks of interacting species^{1–4}. In networks, chains of effects caused by a range of species have an indirect effect on other species they do not interact with directly, potentially affecting the fitness outcomes of a variety of ecological interactions (such as mutualism)^{5–7}. Here we apply analytical techniques and numerical simulations to 186 empirical mutualistic networks and show how both direct and indirect effects alter the fitness of species coevolving in these networks. Although the fitness of species usually increased with the number of mutualistic partners, most of the fitness variation across species was driven by indirect effects. We found that these indirect effects prevent coevolving species from adapting to their mutualistic partners and to other sources of selection pressure in the environment, thereby decreasing their fitness. Such decreases are distributed in a predictable way within networks: peripheral species receive more indirect effects and experience higher reductions in fitness than central species. This topological effect was also evident when we analysed an empirical study of an invasion of pollination networks by honeybees. As honeybees became integrated as a central species within networks, they increased the contribution of indirect effects on several other species, reducing their fitness. Our study shows how and why indirect effects can govern the adaptive landscape of species-rich mutualistic assemblages.

Fitness—the ability of organisms to survive and reproduce—is the fundamental biological currency that underlies the ecology and evolution of biodiversity^{8,9}. Variation in fitness among organisms mediates processes and patterns at multiple scales, from the persistence and evolution of populations to the reorganization and functionality of ecological communities^{10,11}. In nature, much of fitness variation is the outcome of ecological interactions, ranging from antagonism to mutualism^{12–14}. Mutualism is particularly intriguing because some of the most diverse ecosystems, such as coral reefs and tropical forests, are strongly supported by these interactions of mutual benefit¹³. Mutualistic interactions, by definition, increase the fitness of interacting individuals, so they can raise the average fitness across the individuals of a given species¹⁵ (the ‘species fitness’). Fitness increases may be fuelled by reciprocal evolutionary changes in traits (coevolution), which in turn may cascade back and further change species fitness¹⁶. Such fitness–coevolution–trait feedback effects may be altered by interactions with other species within ecological communities^{3,17,18}.

As a result, species fitness may evolve through a combination of direct reciprocal selection on each pair of interacting species and indirect effects mediated by selection acting on species that are not linked directly as interacting partners^{5,18}. These indirect effects, in turn, may create or intensify conflicting selective pressures, thereby reshaping the adaptive landscape and the distribution of species fitness within a network of interactions^{5,19}. This combination of direct and indirect effects may pervade most interaction networks among free-living species, where interactions typically show very low specificity.

Here we use a combination of mathematical modelling and empirical mutualistic networks to understand how indirect effects shape species fitness. Our starting point is a classical discrete time quantitative-genetics equation that describes how a continuous phenotypic trait evolves in response to a selection gradient²⁰ (Methods). In evolutionary biology, a selection gradient describes the relationship between species fitness and a continuous phenotypic trait by dictating the strength and direction of natural selection on the trait²⁰.

¹Programa de Pós-Graduação em Ecologia, Departamento de Ecologia, Instituto de Biociências, Universidade de São Paulo, São Paulo, Brazil. ²Departamento de Genética e Biologia Evolutiva, Instituto de Biociências, Universidade de São Paulo, São Paulo, Brazil. ³Instituto de Física ‘Gleb Wataghin’, Universidade Estadual de Campinas, Campinas, Brazil. ⁴Departamento de Biología Animal, Instituto de Biología, Universidad Estadual de Campinas, Campinas, Brazil. ⁵Island Ecology and Evolution Research Group, Institute of Natural Products and Agrobiology (IPNA-CSIC), San Cristóbal de La Laguna, Spain. ⁶Estación Biológica de Doñana, CSIC, Sevilla, Spain. ⁷Departamento de Biología Vegetal y Ecología, Universidad de Sevilla, Sevilla, Spain. ⁸Department of Ecology and Evolutionary Biology, University of California, Santa Cruz, CA, USA. ⁹Department of Evolutionary Biology and Environmental Studies, University of Zurich, Zurich, Switzerland.

¹⁰Departamento de Ecología, Instituto de Biociências, Universidade de São Paulo, São Paulo, Brazil. ✉e-mail: legiacobelli@gmail.com

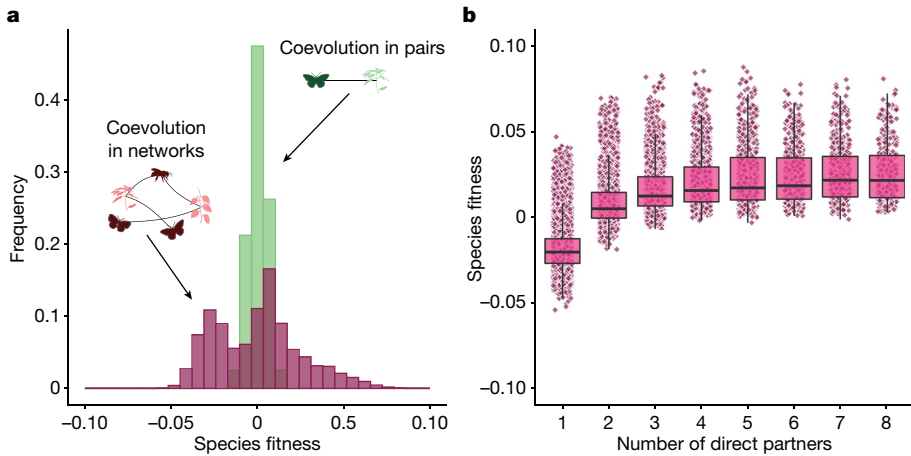


Fig. 1 | Coevolution in mutualistic networks increases variability in species fitness. **a**, Histogram showing the distribution of species fitness (rescaled relative to the average) that coevolved in a single mutualistic pair (green bars) or within the 186 empirical networks used to parameterize the model (purple). **b**, When coevolving within networks, species fitness increased with the number of direct, mutualistic partners up to a saturation point, but it was highly variable among species with the same number of partners. Each fitness

value corresponds to the mean value for 10^3 numerical simulations of our model. In both **a** and **b**, fitness values are rescaled relative to the average of each scenario (coevolution in pairs or in networks) in such a way that zero indicates the average of the distributions in each scenario. In **b**, only species that coevolved in networks are shown. Parameter values are as follows: $m_i = 0.5$, $\sigma_{Gz_i}^2 = 1.0$, $q_i = 0.2$, $\alpha = 0.2$. θ_i and initial trait values were sampled from a uniform distribution $U[0, 10]$.

For mutualistic species, natural selection has at least two distinct sources. First, selection from mutualistic partners favours complementarity of traits, for instance when the proboscis of a butterfly matches the length of the floral tube of plants, or in multi-species assemblages, when a plant trait fits within the range of potential animal partners^{21–23}. The second selective force comes from the environment and other factors unrelated to mutualisms, such as abiotic factors, that favour an optimal trait value for each species (the ‘environmental optima’)^{24–27}. In our coevolutionary model we assumed that these two sources of selective pressure therefore make up the selection gradient and drive the evolution of a species trait (Methods):

$$\bar{z}_i^{(t+1)} = \bar{z}_i^{(t)} + \sigma_{Gz_i}^2 q_i \left[m_i \sum_{j,j \neq i}^N q_{ij}^{(t)} (\bar{z}_j^{(t)} - \bar{z}_i^{(t)}) + (1-m_i) (\theta_i - \bar{z}_i^{(t)}) \right]. \quad (1)$$

Equation (1) relates how the trait of a species (\bar{z}_i) evolves according to the available additive genetic variance on the trait ($\sigma_{Gz_i}^2$), as well as the selection gradient outlined earlier, represented by the other terms in the equation. The first term in the selection gradient, $\sum_{j,j \neq i}^N q_{ij}^{(t)} (\bar{z}_j^{(t)} - \bar{z}_i^{(t)})$, measures the selective pressures coming from each mutualistic partner j , with each partner j favouring trait complementarity with a relative strength $q_{ij}^{(t)}$ (Methods). In turn, the second term, $(\theta_i - \bar{z}_i^{(t)})$, describes the component of the selection gradient that drives the evolution of species traits towards the environmental optima. Other parameters in equation (1) include m_i , which measures the proportional contribution of mutualism as selective pressures, and q_i , which measures the sensitivity of the selection gradient to the different values of trait \bar{z}_i .

The selection gradient corresponds to the slope of the relationship between the natural logarithm of species fitness and mean trait values, $\frac{d \ln W_i}{d \bar{z}_i}$. Therefore, it is possible to integrate the selection gradient to derive the fitness of each species as a function of trait values. Using this approach, we derived the fitness function that underlies our coevolutionary model:

$$\overline{W}_i = e^{\frac{1}{2} q_i \left[\frac{m_i}{\alpha} \ln \left(\frac{s_i}{k_i} \right) - (1-m_i) (\theta_i - \bar{z}_i)^2 \right]}. \quad (2)$$

Equation (2) represents the fitness of a given species i relative to its theoretical maximum fitness and describes the relationship between

a species’ phenotypic trait (represented by \bar{z}_i) and its fitness. Thus, $0 < \overline{W}_i \leq 1$, the upper bound corresponding to the case of species i achieving the maximum possible fitness for a species with the same number of mutualistic partners (Methods).

The function described in equation (2) shows that species fitness depends on two main components, each representing a different aspect of the fitness landscape. First, it depends on a mutualistic component in which fitness increases with the average trait matching of species across its mutualistic partners, s_i/k_i . The term $s_i = \sum_{j=1, j \neq i}^N a_{ij} e^{-\alpha(\bar{z}_j - \bar{z}_i)^2}$ represents the total trait matching with all j mutualistic partners, and $k_i = \sum_{j=1, j \neq i}^N a_{ij}$ is the total number of mutualistic partners of species i ($a_{ij} = 1$ if species i interacts with species j , otherwise $a_{ij} = 0$). The parameter α controls the sensitivity of trait matching to differences in the trait values of mutualistic partners. The second component, represented by $(\theta_i - \bar{z}_i)^2$, describes the squared distance between a species’ trait value and the environmental optimum, θ_i . The less distant species traits are from their environmental optima, the greater the fitness is. Therefore, species achieve the maximum possible fitness ($\overline{W}_i = 1$) when their traits perfectly match the traits of all their mutualistic partners and the environmental optimum (Methods).

Using the fitness function and our coevolutionary model, we first explored how coevolving in a mutualistic network affects species fitness. We performed numerical simulations of our model parameterized with the structure of 186 empirical networks, encompassing a wide range of network topologies and types of mutualism worldwide (Methods). The coevolutionary dynamics quickly reached a global stable equilibrium in which traits and, consequently, species fitness ceased to change (Methods and Extended Data Fig. 1). Trait values and species fitness at equilibrium are analytically predictable, even if not all species are guaranteed to persist throughout the coevolutionary dynamics (Extended Data Fig. 1 and Supplementary Methods). At equilibrium, the fitness of species that coevolved in networks varied 5 times as much as the fitness of isolated pairs of coevolved species (s.d. = 0.025 in networks versus 0.005 in pairs; Fig. 1a). This increased variation in the fitness of species that coevolved within networks was due in part to the number of direct partners. Species fitness was higher for species with two or more direct partners than for species in the network that interacted with only one direct partner, leading to a bimodal distribution of fitness values (Fig. 1a,b). The greater variability in fitness for species that coevolve in mutualistic networks holds under a wide range of scenarios

in which other ecological processes may drive species with low fitness extinct and the extant species coevolve to a new equilibrium (Extended Data Fig. 2 and Supplementary Methods). Furthermore, the bimodality in the distribution of species fitness becomes less noticeable as the number of extinctions increases, but only disappears when the number of extinctions exceeds 40% of species in the network (Extended Data Fig. 2 and Supplementary Methods). The increase in fitness for species with two or more partners was expected and occurs because having a larger number of partners evens out differences in the contribution to fitness of individual mutualistic partner species, increasing fitness through geometric mean effects^{28–31} (Supplementary Methods). Even so, the effects of the number of partners quickly saturated and only partly explained the variability in species fitness (Fig. 1b), indicating that indirect effects have a potential role in shaping fitness variation across species.

After quantifying the overall effects of coevolution in networks for species fitness and identifying the potential importance of indirect effects, we next derived an analytical approximation that explicitly assesses how indirect evolutionary effects shape the fitness of species that coevolve within networks (Supplementary Methods). By combining the fitness function (equation (2)) and the equation for species' traits at coevolutionary equilibrium (Methods), we obtained the following approximation:

$$\bar{w}_i^* \cong e^{-\frac{1}{2} q_i \{ m_i [(\langle \theta \rangle - \theta_i)(m_i + F_i) - \theta_i + \langle z \rangle]^2 + (1-m_i)(\theta_i - \langle \theta \rangle)^2(m_i + F_i)^2 \}} \quad (3)$$

where \bar{w}_i^* is the fitness of species i at the coevolutionary equilibrium, $\langle \theta \rangle$ represents the mean environmental optimum across all species other than i in the network, $\langle z \rangle$ is the average trait value across mutualistic partners of i , and F_i represents the proportional contribution of indirect evolutionary effects to the evolution of species i .

Our analytical approximation showed that indirect evolutionary effects prevent coevolving species from simultaneously achieving high trait matching with mutualistic partners and trait values favoured by environmental selection. Thus the larger the contribution of indirect effects generated by other species to the evolution of a given species i , the smaller the fitness of i (Fig. 2a). Our analytical results also showed that the contribution of indirect effects is strongly affected by network structure: indirect effects are minimized if a species is the central species of a network, whereas peripheral species are affected more by indirect effects. This increased influence of indirect effects means that the fitness of peripheral species is lower than the fitness of central species (Supplementary Methods).

The relationship between species fitness and indirect effects was strong and held for numerical simulations that relaxed the simplifying assumptions of our analytical approximation (Fig. 2a–c) and incorporated the network structure of empirical mutualism. Sensitivity analyses further indicated that the role of indirect effects in species fitness substantially weakens only when mutualistic selection is either very weak or very strong, or when the environmental optima of species are very narrowly distributed in the network ($m_i \leq 0.1$ or $m_i \geq 0.9$; Extended Data Figs. 3–5 and Supplementary Methods). Furthermore, the way in which indirect evolutionary effects shape fitness holds even when the species with the lowest fitness become extinct, for instance, because of the ecological dynamics of the system (Extended Data Fig. 6 and Supplementary Methods). Except at these extreme values of m_i , indirect evolutionary effects can strongly shape species fitness within coevolving mutualistic networks. These extremes are not expected to be common in nature, for two reasons. First, we have evidence that the selection imposed on species' traits by mutualistic interactions and other sources in the environment are similar in strength to each other, even for highly intimate types of mutualism, such as symbiosis^{32–35}. Second, mutualistic networks are composed of different organisms, each with its own life history and developmental constraints. In turn, species' life history and developmental constraints can be radically

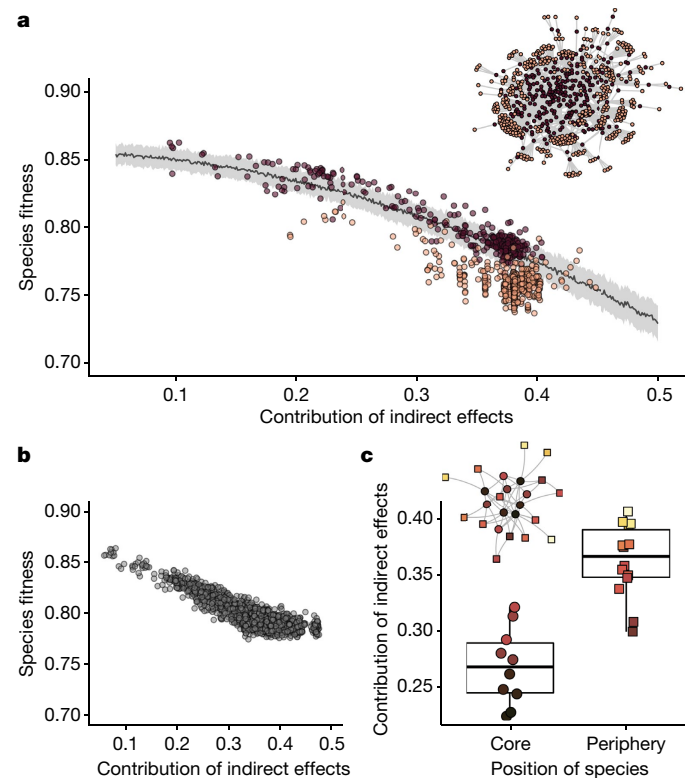
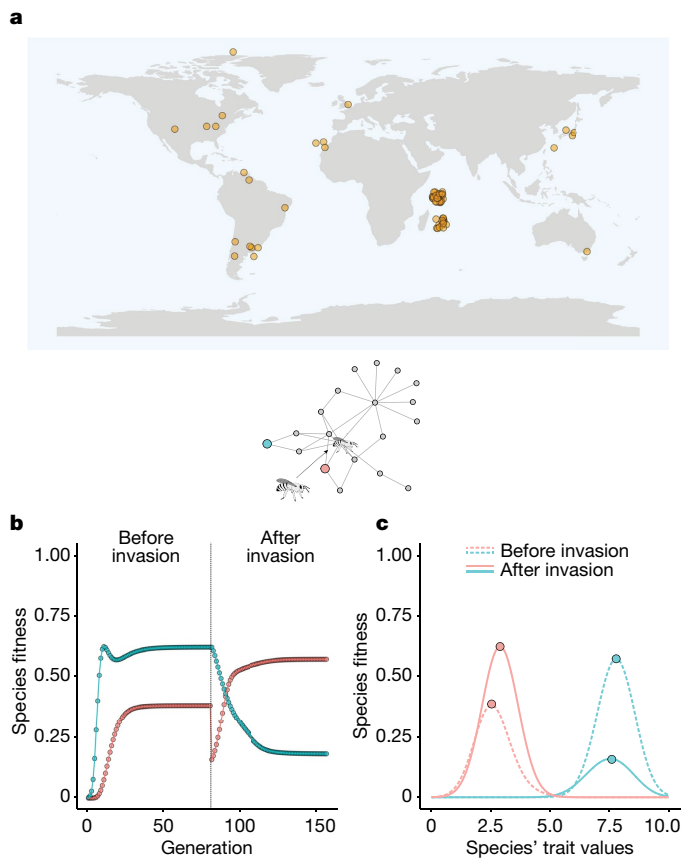


Fig. 2 | The position of species within networks and indirect evolutionary effects shape species fitness in coevolved mutualistic networks. **a**, An analytical approximation (solid curve and shaded region) predicts that indirect evolutionary effects decrease the fitness of species coevolving in mutualistic networks. The data points represent species with either one partner (light colours) or more than one (darker dots). This effect held for numerical simulations ($n = 10^3$ numerical simulations for each of the 186 empirical networks), as shown, for example, for species in a plant–pollinator network (inset). **b**, This effect also held for species across all empirical networks after controlling for the effects of the number of mutualistic partners. The graph shows species with three partners across all networks. **c**, Example of a seed-dispersal network (inset) showing how species in peripheral positions receive more indirect effects and have lower fitness than core species. The colour of points represents species fitness: the darker the colour, the higher the fitness. In **a**, the line represents the mean predicted fitness, and shaded regions show standard deviations when sampling species' environmental optima (θ_i and $\langle \theta \rangle$) and $\langle z \rangle$ from a normal distribution; $\theta_i \sim N(0.0, 0.1)$, $\langle \theta \rangle \sim N(2.5, 0.1)$ and $\langle z \rangle \sim N(2.5, 0.1)$. Points correspond to the mean value of species fitness (**a** and **b**) or the contribution of indirect effects (**c**) across 10^3 numerical simulations. Other parameter values are as follows: $m_i = 0.5$, $\sigma_{Gz_i}^2 = 1.0$, $q_i = 0.2$ and $\alpha = 0.2$. For numerical simulations, θ_i and initial trait values were sampled from a uniform distribution $U[0, 10]$. In **a** and **b**, the x axis represents the proportional contribution of indirect evolutionary effects (equation (3)).

different among species and can shape how traits respond to selection¹². Our results therefore indicate that indirect evolutionary effects should have a pervasive role in shaping the fitness of mutualistic species in ecological communities.

Human activities that homogenize ecological communities can lead to a reorganization of direct and indirect interactions, ultimately changing the outcome of coevolution and altering species fitness^{27,36–38}. One important example would be the introduction of a new species into a network. As a case study, we explored the potential consequences of the reorganization of direct and indirect effects by the introduction of the European honeybee (*Apis mellifera*), which often becomes a central species in pollination networks worldwide^{39–42}. We first performed numerical simulations on 73 empirical networks that include *A. mellifera* (Fig. 3a and Methods) by first removing it from the network



and running the coevolutionary model until it reached equilibrium. We then connected *A. mellifera* back to the network to simulate an invasion and evaluated how the fitness of all the other native species was affected after reaching a new equilibrium. This approach allowed us to use our controlled scenario as a theoretical benchmark. Nevertheless, this certainly represents a simplistic assumption because it neglects the reduction in the number of species, mutualistic interactions and the potential rewiring of native pollinators after the invasion. We will relax these assumptions later by considering a field experiment involving a pollination network both before and after the introduction of *A. mellifera* by beekeeping practices³⁹.

Our simulations show that invasive species such as *A. mellifera* can substantially affect the fitness of native species (Fig. 3b) and reshape their adaptive landscapes (Fig. 3c). Specifically, we found that the effects of the invasion differed between species that interact directly with honeybees and those that interact only indirectly. The fitness of the honeybee's direct partners increased on average after the invasion ($n = 10^3$ simulations; Fig. 4a), whereas for species that interact only indirectly with the honeybee, the overall effect on fitness was negative ($n = 10^3$ simulations; Fig. 4a). In our simulations, the average change in fitness was positive only if the increase in fitness of gaining a new mutualistic partner (the honeybee) compensated for the decrease in

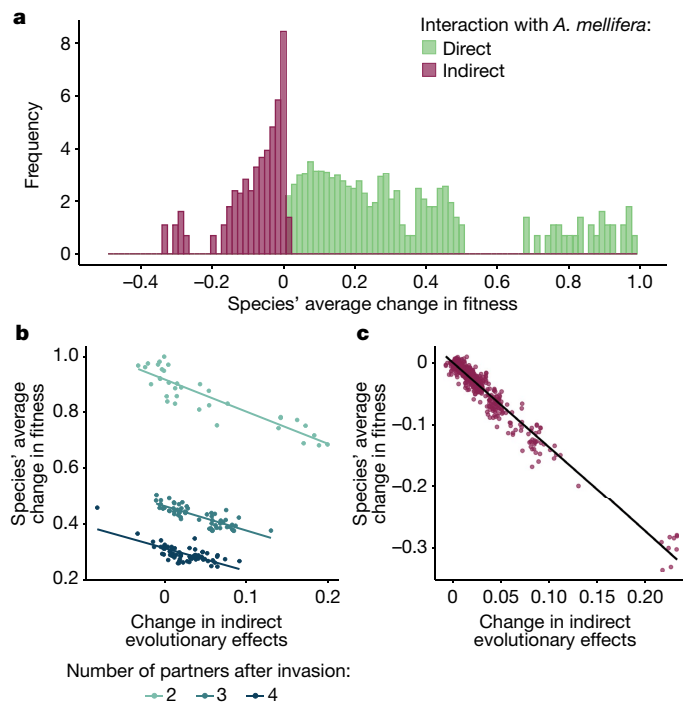


Fig. 4 | Indirect evolutionary effects shape the fitness consequences of simulated network invasions. **a**, The average change in species fitness (across all 10^3 simulations) after coevolving with an invasive species. The frequency represents $\log(\text{counts})$. **b,c**, Relationship between the average change in species fitness after the invasion, and the change in the total contribution of indirect evolutionary effects coming from the network for direct (**b**) partners and indirect (**c**) partners of the invasive species. Points and histogram bars represent the average values across all simulations ($n = 10^3$ numerical simulations, 73 networks). The x axis in **a** and the y axis in **b,c** are rescaled relative to the maximum absolute value of average change in fitness across all species. Parameter values are as follows: $m_i = 0.5$, $\sigma_{Gz_i}^2 = 1.0$, $q_i = 0.2$, $\alpha = 0.2$. θ_i and initial trait values were sampled from a uniform distribution $U[0, 10]$.

fitness caused by changes in indirect evolutionary effects (Fig. 4b). In contrast, for species that interact only indirectly with the honeybee, fitness decreased because the invasion increased the contribution of indirect evolutionary effects to the fitness of these species (Fig. 4c). As our results above showed, increasing the contribution of indirect evolutionary effects reduces species fitness because it hinders the ability of species to adapt at the same time to both mutualistic partners and the environment. These results held for different values of mutualistic selection (Extended Data Figs. 7–9 and Supplementary Methods).

However, when *A. mellifera* invades a network in nature, some native pollinators become disconnected from the network (that is, they become functionally extinct), and those left in the system rewire their interactions and lose mutualistic partners through resource competition³⁹. We explored these additional consequences using the data from an experimental field study in which the mutualistic networks before and after the arrival of *A. mellifera* are available³⁹. These simulations showed that the fitness of 68% of the native species decreased after the introduction of *A. mellifera* because the honeybee not only increased the contribution of indirect evolutionary effects, but it also drastically reduced the number of mutualistic partners for nearly all the native plant species in the network (Extended Data Fig. 10). Together with our theoretical benchmark, these results indicate that mutualistic interactions with an invasive species can decrease the fitness of most native species in networks by reorganizing the indirect evolutionary effects. Despite this, the negative effects on fitness can be buffered if species are able to obtain new mutualistic partners with similar effectiveness after

the invasion, but the experimental evidence indicates that this would rarely be the case, especially at high densities of the invader species³⁹.

Our results indicate that mutualists coevolve in a dynamic ‘seascape’ within which adaptive peaks can be transient and cause natural selection to push mutualists to lower or higher fitness points, depending on the structure and reorganization of indirect evolutionary effects⁴³. Specifically, indirect effects resulting from coevolution constrain species fitness. We therefore predict that selection may favour the evolution of lifestyles that reduce the negative impact of indirect evolutionary effects, especially in species-rich assemblages with low interaction specificity. Two examples are specialists with a high dependency on mutualisms and supergeneralists. For these specialists, their dependence on mutualistic interactions is so high that it minimizes how indirect evolutionary effects create conflicting selective pressures with the environment and negatively impact fitness. Supergeneralists rely on resources provided directly by multiple partners, so their fitness is less affected by indirect effects, thereby maximizing the contribution of direct effects over indirect ones^{1,18}. Furthermore, when supergeneralists invade native communities, this may reduce the fitness of mutualists through indirect evolutionary effects, an often-overlooked outcome of biological invasions. Moreover, a generalized effect of environmental drivers (such as the effects of climate change on pollinators) may strongly influence both the sign and the magnitude of indirect effects, translating to larger fitness losses among species. More generally, our results highlight how and why the structure of ecological networks can govern the fitness, the adaptive landscape and, consequently, the persistence of species across Earth’s ecosystems.

Online content

Any methods, additional references, Nature Portfolio reporting summaries, source data, extended data, supplementary information, acknowledgements, peer review information; details of author contributions and competing interests; and statements of data and code availability are available at <https://doi.org/10.1038/s41586-023-06319-7>.

- Thompson, J. N. The coevolving web of life. *Am. Nat.* **173**, 125–140 (2009).
- Thompson, J. N. Mutualistic webs of species. *Science* **312**, 372–373 (2006).
- Bascompte, J. & Jordano, P. Plant–animal mutualistic networks: the architecture of biodiversity. *Annu. Rev. Ecol. Evol. Syst.* **38**, 567–593 (2007).
- Bascompte, J. Disentangling the web of life. *Science* **325**, 416–419 (2009).
- Guimarães, P. R. Jr, Pires, M. M., Jordano, P., Bascompte, J. & Thompson, J. N. Indirect effects drive coevolution in mutualistic networks. *Nature* **550**, 511–514 (2017).
- Wootton, J. T. The nature and consequences of indirect effects in ecological communities. *Annu. Rev. Ecol. Syst.* **25**, 443–466 (1994).
- Strauss, S. Y. Indirect effects in community ecology: their definition, study and importance. *Trends Ecol. Evol.* **6**, 206–210 (1991).
- Darwin, C. *On the Origin of Species by Means of Natural Selection, or the Preservation of Favoured Races in the Struggle for Life* (Murray, 1861).
- Fisher, R. A. *The Genetical Theory of Natural Selection* (Clarendon Press, 1930).
- Reed, D. H. Relationship between population size and fitness. *Conserv. Biol.* **19**, 563–568 (2005).
- Orr, H. A. Fitness and its role in evolutionary genetics. *Nat. Rev. Genet.* **10**, 531–539 (2009).
- Thompson, J. N. *Relentless Evolution* (Univ. Chicago Press, 2013).
- Bronstein, J. L. *Mutualism* (Oxford Univ. Press, 2015).
- Bronstein, J. L. Our current understanding of mutualism. *Q. Rev. Biol.* **69**, 31–51 (1994).
- Bronstein, J. L., Dieckmann, U. & Ferrière, R. in *Evolutionary Conservation Biology* (eds Ferrière, R. et al.) 305–326 (Cambridge Univ. Press, 2009).

- Thompson, J. N. *The Geographic Mosaic of Coevolution* (Univ. Chicago Press, 2005).
- Nuismer, S. L., Jordano, P. & Bascompte, J. Coevolution and the architecture of mutualistic networks. *Evolution* **67**, 338–354 (2013).
- Guimarães, P. R. Jr, Jordano, P. & Thompson, J. N. Evolution and coevolution in mutualistic networks. *Ecol. Lett.* **14**, 877–885 (2011).
- Kauffman, S. A. & Johnsen, S. Coevolution to the edge of chaos: coupled fitness landscapes, poised states, and coevolutionary avalanches. *J. Theor. Biol.* **149**, 467–505 (1991).
- Lande, R. Natural selection and random genetic drift in phenotypic evolution. *Evolution* **30**, 314–334 (1976).
- Santamaría, L. & Rodríguez-Gironés, M. A. Linkage rules for plant–pollinator networks: trait complementarity or exploitation barriers? *PLoS Biol.* **5**, e31 (2007).
- Rohr, R. P., Naisbit, R. E., Mazza, C. & Bersier, L.-F. Matching–centrality decomposition and the forecasting of new links in networks. *Proc. R. Soc. B* **283**, 20152702 (2016).
- Peralta, G. et al. Trait matching and phenological overlap increase the spatio-temporal stability and functionality of plant–pollinator interactions. *Ecol. Lett.* **23**, 1107–1116 (2020).
- Galen, C. High and dry: drought stress, sex-allocation trade-offs, and selection on flower size in the alpine wildflower *Polemonium viscosum* (Polemoniaceae). *Am. Nat.* **156**, 72–83 (2000).
- Irwin, R. E., Adler, L. S. & Brody, A. K. The dual role of floral traits: pollinator attraction and plant defense. *Ecology* **85**, 1503–1511 (2004).
- Strauss, S. Y. & Whittall, J. B. in *Ecology and Evolution of Flowers* (eds Harder, L. D. & Barrett, S. C. H.) 120–138 (Oxford Univ. Press, 2006).
- Galetti, M. et al. Functional extinction of birds drives rapid evolutionary changes in seed size. *Science* **340**, 1086–1090 (2013).
- Yoshimura, J. & Janzen, V. A. A. Evolution and population dynamics in stochastic environments. *Res. Popul. Ecol.* **38**, 165–182 (1996).
- Bascompte, J., Possingham, H. & Roughgarden, J. Patchy populations in stochastic environments: critical number of patches for persistence. *Am. Nat.* **159**, 128–137 (2002).
- Waser, N. M., Chittka, L., Price, M. V., Williams, N. M. & Ollerton, J. Generalization in pollination systems, and why it matters. *Ecology* **77**, 1043–1060 (1996).
- Levins, R. The effect of random variations of different types on population growth. *Proc. Natl Acad. Sci. USA* **62**, 1061–1065 (1969).
- Piculell, B. J., Hoeksema, J. D. & Thompson, J. N. Interactions of biotic and abiotic environmental factors in an ectomycorrhizal symbiosis, and the potential for selection mosaics. *BMC Biol.* **6**, 23 (2008).
- Batstone, R. T., Peters, M. A. E., Simonsen, A. K., Stinchcombe, J. R. & Frederickson, M. E. Environmental variation impacts trait expression and selection in the legume–rhizobium symbiosis. *Am. J. Bot.* **107**, 195–208 (2020).
- Caruso, C. M., Eisen, K. E., Martin, R. A. & Sletvold, N. A meta-analysis of the agents of selection on floral traits. *Evolution* **73**, 4–14 (2019).
- Munguía-Rosas, M. A., Ollerton, J., Parra-Tabla, V. & De-Nova, J. A. Meta-analysis of phenotypic selection on flowering phenology suggests that early flowering plants are favoured. *Ecol. Lett.* **14**, 511–521 (2011).
- Fricke, E. C. & Svensson, J.-C. Accelerating homogenization of the global plant–frugivore meta-network. *Nature* **585**, 74–78 (2020).
- Mackin, C. R., Peña, J. F., Blanco, M. A., Balfour, N. J. & Castellanos, M. C. Rapid evolution of a floral trait following acquisition of novel pollinators. *J. Ecol.* **109**, 2234–2246 (2021).
- Stuart, Y. E. et al. Rapid evolution of a native species following invasion by a congener. *Science* **346**, 463–466 (2014).
- Valido, A., Rodríguez-Rodríguez, M. C. & Jordano, P. Honeybees disrupt the structure and functionality of plant–pollinator networks. *Sci. Rep.* **9**, 4711 (2019).
- Aizen, M. A., Morales, C. L. & Morales, J. M. Invasive mutualists erode native pollination webs. *PLoS Biol.* **6**, e31 (2008).
- Traveset, A. & Richardson, D. M. Mutualistic interactions and biological invasions. *Annu. Rev. Ecol. Evol. Syst.* **45**, 89–113 (2014).
- Traveset, A. & Richardson, D. M. Biological invasions as disruptors of plant reproductive mutualisms. *Trends Ecol. Evol.* **21**, 208–216 (2006).
- Merrel, D. J. *The Adaptive Seascape: The Mechanism of Evolution* (Univ. Minnesota Press, 1994).

Publisher's note Springer Nature remains neutral with regard to jurisdictional claims in published maps and institutional affiliations.

Springer Nature or its licensor (e.g. a society or other partner) holds exclusive rights to this article under a publishing agreement with the author(s) or other rightsholder(s); author self-archiving of the accepted manuscript version of this article is solely governed by the terms of such publishing agreement and applicable law.

© The Author(s), under exclusive licence to Springer Nature Limited 2023

Article

Methods

Modelling coevolution in mutualistic networks

The starting point of our model is a classic quantitative-genetics equation²⁰ that relates how the mean value of a continuous trait (\bar{z}_i) of a species changes between successive generations in response to the selection pressures in the environment:

$$\Delta \bar{z}_i = \sigma_{Gz_i}^2 \frac{d \ln \bar{W}_i^{(t)}}{d \bar{z}_i^{(t)}} \quad (4)$$

where $\sigma_{Gz_i}^2$ is the additive genetic variance of trait z_i . The term $\frac{d \ln \bar{W}_i^{(t)}}{d \bar{z}_i^{(t)}}$ is the selection gradient and connects how changes in z_i affect the mean fitness of species i . In natural communities, the traits of a species that engages in mutualistic interactions are subject to the selection pressures of the species it interacts with and other sources in the environment. We therefore assumed that the selection gradient, $\frac{d \ln \bar{W}_i^{(t)}}{d \bar{z}_i^{(t)}}$, is composed of two sources of selection pressure. First, we assumed that for a given species i , mutualism contributes to a proportion, m_i , of the evolution of trait \bar{z}_i . Following empirical evidence and previous work^{5,26,27,44}, we further assumed: that mutualistic interactions of species i with each partner j favour trait complementarity (such as the complementarity between insect mouthparts and the floral tubes of plants); and that each mutualistic partner j of species i contributes a given amount ($q_{ij}^{(t)}$) to the selection pressures that act on trait \bar{z}_i . We also assumed that the selection pressures from other features of the environment, such as abiotic factors, contribute to the remaining portion ($1 - m_i$) of the evolution of trait \bar{z}_i and favour an optimal trait value (the ‘environmental optima’, θ_i). Given these assumptions, the selection gradient, $\frac{d \ln \bar{W}_i^{(t)}}{d \bar{z}_i^{(t)}}$, can be described as:

$$\frac{d \ln \bar{W}_i^{(t)}}{d \bar{z}_i^{(t)}} = q_i \left[m_i \sum_{j=1, j \neq i}^N q_{ij}^{(t)} (\bar{z}_j^{(t)} - \bar{z}_i^{(t)}) + (1 - m_i) (\theta_i - \bar{z}_i^{(t)}) \right] \quad (5)$$

where q_i is a constant that measures the sensitivity of species fitness to changes in the values of $\bar{z}_i^{(t)}$. The term $q_{ij}^{(t)}$ quantifies the evolutionary contribution of a given mutualistic partner j to the selection imposed on $\bar{z}_i^{(t)}$. We assumed that $q_{ij}^{(t)}$ depends on a trait-matching rule such that $q_{ij}^{(t)}$ increases with the trait matching between species i and a partner j , relative to all other k partners of i :

$$q_{ij}^{(t)} = \frac{a_{ij} e^{-\alpha (\bar{z}_j^{(t)} - \bar{z}_i^{(t)})^2}}{\sum_{k=1, k \neq i}^N a_{ik} e^{-\alpha (\bar{z}_k^{(t)} - \bar{z}_i^{(t)})^2}} \quad (6)$$

in which a_{ij} (a_{ik}) = 1 if species i interacts with species j (k) in the network or equals 0 otherwise; and α is a parameter that controls the sensitivity of $q_{ij}^{(t)}$ to the distance between species traits. Combining equations (4)–(6) results in our coevolutionary model, equation (1).

Linking coevolution and species fitness

In our model, the selection gradient, $\frac{d \ln \bar{W}_i}{d \bar{z}_i}$, connects the evolution of species traits to how mutualism and the environment affect their mean fitness⁵. To derive the expression that explicitly links coevolution to species’ mean fitness, $\bar{W}_i(\bar{z}_i)$, we solved equation (5) to obtain species’ absolute fitness (Supplementary Methods). Assuming a selection gradient first, and then integrating it to find fitness, results in an equation that describes an entire family of fitness functions that could lead to the same selection gradient (see Supplementary Methods for more examples):

$$\bar{W}_i = e^{q_i \left[\frac{m_i}{2\alpha} \ln \left(\sum_{j=1, j \neq i}^N a_{ij} e^{-\alpha (\bar{z}_j - \bar{z}_i)^2} \right) + (1 - m_i) \left(\theta_i - \frac{\bar{z}_i^2}{2} \right) \right] + c_i} \quad (7)$$

where c_i is a constant that emerges from the integration of the selection gradient. Thus, instead of a specific function, equation (7) is a general

representation of an entire family of fitness functions, depending on the choice of the constant c_i . It can be shown that equation (7) can lead to other fitness functions used in previous work by choosing different values for c_i (Supplementary Methods). Because in equation (7) species fitness scales up with the number of mutualistic partners with the value of the environmental optima (θ_i), and depends on an arbitrary constant (c_i), we performed two additional steps. First, we found the conditions under which species achieve their maximum theoretical absolute fitness. The absolute fitness of species will be maximized whenever species are at their adaptive peaks (that is, when $\frac{d \ln \bar{W}_i}{d \bar{z}_i} = 0$). From equation (5), because $0 < m_i < 1$, this condition is fulfilled when $\bar{z}_i = \bar{z}_j$ for all mutualistic partners j , and, at the same time, $\bar{z}_i = \theta_i$ (except for the trivial case in which $q_i = 0$). Thus fitness is maximized when species are perfectly adapted to all mutualistic partners and to the environmental optima (that is, when all species share the same environmental optima). Putting this condition into equation (7) yields:

$$\bar{W}_{\max,i} = e^{q_i \left[\frac{m_i}{2\alpha} \ln \left(\sum_{j=1, j \neq i}^N a_{ij} \right) + (1 - m_i) \left(\frac{\theta_i^2}{2} \right) \right] + c_i}. \quad (8)$$

Next, we computed species’ relative fitness (\bar{w}_i) as the ratio $\frac{\bar{W}_i}{\bar{W}_{\max,i}}$, resulting in equation (2), which indicates how close the species is to the maximum fitness value for a species with the same number of partners.

Linking indirect evolutionary effects to species fitness

Our coevolutionary model always leads to a stable equilibrium of species’ traits (and therefore species fitness). Using the simplifying assumption that $q_{ij}^{(t)} \approx q_{ij}$ from equation (1), species traits reach a coevolutionary equilibrium when:

$$m_i \sum_{j=1, j \neq i}^N q_{ij} (\bar{z}_j^* - \bar{z}_i^*) + (1 - m_i) (\theta_i - \bar{z}_i^*) = 0 \quad (9)$$

Equation (9) leads to:

$$\bar{z}_i^* - m_i \sum_{j=1, j \neq i}^N q_{ij} \bar{z}_j^* = (1 - m_i) \theta_i, \quad (10)$$

and equation (10) can be rewritten in matrix form as:

$$\mathbf{Z}^* - Q \mathbf{Z}^* = \psi \boldsymbol{\Theta}, \quad (11)$$

$$\mathbf{Z}^* = (I - Q)^{-1} \psi \boldsymbol{\Theta}. \quad (12)$$

In equations (11) and (12), \mathbf{Z}^* is an $N \times 1$ vector of species’ traits at the coevolutionary equilibrium, ψ is an $N \times N$ diagonal matrix with $1 - m_i$ as its diagonal elements; $\boldsymbol{\Theta}$ is an $N \times 1$ vector of species’ environmental optima (θ_i); and I is the identity matrix. The Q matrix is a matrix in which the entries, $m_i q_{ij}$, contain the direct evolutionary effects between species i and j .

$T = (I - Q)^{-1}$ is a matrix that contains not only the direct but also the indirect evolutionary effects that come from the multiple pathways connecting species in the network. This interpretation can be recovered by noticing that the T matrix is the result of a matrix power series:

$$(I - Q)^{-1} = Q^0 + Q^1 + Q^2 + Q^3 \dots = \sum_{\ell=0}^{\infty} Q^\ell. \quad (13)$$

The powers of the Q matrix in equation (13) correspond to matrices that represent the effects of species on each other through multiple pathways in the network. Thus, although the Q matrix represents the direct evolutionary effects that species exert on each other, each power ℓ of the Q matrix contains the effects that species j exert on species i through a chain of effects of length ℓ . For instance, the

elements $q_{ij}^{(2)}$ of the matrix Q^2 contains the effects of species j on species i through pathways of length 2, such as the indirect evolutionary effect of one plant species on another plant mediated by a shared animal mutualist. Consequently, the T matrix contains the sum of the evolutionary effects among species flowing through all possible pathways in the network. Using the T matrix, we first partitioned the contribution of indirect evolutionary effects from the direct ones. Then combining equation (12) with the fitness function allowed us to express species fitness as a function of the total amount of incoming evolutionary effects for each species (Supplementary Methods) and to partition the contribution of direct and indirect evolutionary effects to fitness.

Numerical simulations

We evaluated how mutualistic coevolution in ecological networks is connected to species' average fitness by combining numerical simulations and an analytical approximation of our coevolutionary model. These simulations were parameterized with the structure of 186 empirical networks (Supplementary Table 1). Our dataset comprised 186 empirical networks distributed among three types of mutualism: plants with extrafloral nectaries that are protected by ants ($n = 4$); animals that consume the fleshy fruits of plants and disperse their seeds ($n = 34$); and plants with flowers that are pollinated by animals ($n = 148$). These mutualistic interactions span a wide range of network structures of multiple-partner mutualism. All these networks were obtained from the Web of Life database (www.web-of-life.es). Here we focus on mutualism in which there are two distinct sets of species, forming bipartite networks, but other types of mutualism that do not form bipartite networks can also be used to parameterize our coevolutionary model⁴⁵. Examples of such mutualism include Müllerian mimetic rings in which unpalatable species display a warning signal and indirectly benefit each other by a decreased per capita attack rate from predators⁴⁵. In simulations with the same network, we parameterized a_{ij} as 1 if species i and j interacted and 0 otherwise. Furthermore, initial trait values (\bar{z}_i) and environmental optimum values (θ_i) were sampled from a uniform distribution $U[0, 10]$. We sampled environmental optimum values from a uniform distribution because, in mutualistic communities, species can differ widely in terms of life history, physiological constraints and, as a result, environmental optima¹². With this approach we did not assume any particular shape for the distribution of environmental optima of species because, in a uniform distribution, all values occur with the same frequency (they are equiprobable). However, our analytical approximation shows that our results do not rely on a particular distribution for the environmental optima of species, and we also present the results of numerical simulations in which the sampling range of the environmental optimum is narrower than the interval used in the main text (Extended Data Fig. 4b).

All other parameters were held constant and were the same for all species ($\sigma_{Gz_i}^2 = 1.0$, $q_i = 0.2$ and $\alpha = 0.2$). We ran 1,000 simulations for each combination of network and m_i value ($m_i = 0.1, 0.2, 0.3, 0.4, 0.5, 0.6, 0.7, 0.8$ and 0.9) in which we first allowed species' traits to achieve asymptotic values (defined as $|z_i^{(t+1)} - z_i^{(t)}| < 10^{-4}$). We then used these asymptotic trait values in equation (2) to compute the fitness of each species. In the main text we presented the results for the scenario in which $m_i = 0.5$ because in empirical ecological communities the selection pressures from mutualistic interactions and other sources in the environment have been shown to be similar in strength to each other^{24,26,34,35}. However, we also present the results of the numerical simulations for all other m_i values (Extended Data Figs. 3 and 4 and Supplementary Methods).

We used these numerical simulations to test the predictions of our analytical approximations (Supplementary Methods). From the results of our numerical simulations, we built the matrix of total evolutionary effects, the T matrix, $T = (I - Q)^{-1}$. In our model, the T matrix is an $N \times N$ matrix containing the total evolutionary effects among all

N species in a network that determines the trait values of species at the coevolutionary equilibrium (equation (12)). The matrix of direct evolutionary effects (the Q matrix) was built using species' trait values at the coevolutionary equilibrium. Following previous work¹⁸, we used the entries of the T matrix, t_{ij} , to calculate the contribution of indirect evolutionary effects to trait evolution as:

$$F_i = \frac{\sum_{j=1, j \neq i}^N (1 - a_{ij}) t_{ij}}{\sum_{j=1, j \neq i}^N t_{ij}} \quad (14)$$

where F_i is the contribution of indirect evolutionary effects to species i and $a_{ij} = 1$ if species i interacts with species j , and $a_{ij} = 0$ otherwise. All numerical simulations were performed using the Julia programming language⁴⁶ and figures were produced in R⁴⁷. The code to perform numerical simulations and reproduce our results is publicly available⁴⁸.

Numerical simulations exploring the invasion of a supergeneralist species

To evaluate how an introduced supergeneralist species shapes the fitness of the native species, we performed numerical simulations parameterized with a subset of the networks we used ($n = 73$ empirical networks; Supplementary Table 2). These empirical networks were used because they were collected from ecological communities in which the European honeybee, *A. mellifera*, is not a native species. This species is a known supergeneralist that interacts with many species within networks. To simulate how the fitness of species changes after coevolving with the invader, we proceeded as follows. First, we created a 'pre-invasion' network by completely disconnecting *A. mellifera* from the network. We used this pre-invasion network to simulate the coevolutionary dynamics of species before the invasion, allowed species' traits to reach asymptotic values (defined as $|z_i^{(t+1)} - z_i^{(t)}| < 10^{-4}$ for all species) and used equation (2) to calculate species' fitness at these asymptotic values. Second, we 'reintroduced' *A. mellifera* into the network, simulated the coevolutionary dynamics with the resulting 'post-invasion' network, allowed species traits to reach asymptotic values, and calculated species fitness again. Then, using the values for species fitness resulting from coevolution in the pre- and post-invasion networks, we evaluated how species fitness changed as a result of the *A. mellifera* invasion. Indirect evolutionary effects for the pre- and post-invasion networks were calculated using equation (14). For all numerical simulations, initial trait values and environmental optimum values were sampled from a uniform distribution $U[0, 10]$. All other parameters were held constant and were the same for all species ($\sigma_{Gz_i}^2 = 1.0$, $q_i = 0.2$ and $\alpha = 0.2$). For each combination of network and values of m_i ($m_i = 0.1, 0.2, 0.3, 0.4, 0.5, 0.6, 0.7, 0.8$ and 0.9), we ran 10^3 numerical simulations (Extended Data Figs. 7–9 and Supplementary Methods for sensitivity analyses).

Reporting summary

Further information on research design is available in the Nature Portfolio Reporting Summary linked to this article.

Data availability

The dataset of empirical networks used in this study is available in a GitHub repository (https://github.com/lcosmo/Cosmo_et_el_indirect_effects_fitness), in Zenodo (<https://doi.org/10.5281/zenodo.7945239>) and in the Web of Life database (www.web-of-life.es).

Code availability

All the code to perform the numerical simulations used in this study is available in a GitHub repository (https://github.com/lcosmo/Cosmo_et_el_indirect_effects_fitness) and in Zenodo (<https://doi.org/10.5281/zenodo.7945239>).

Article

44. Nuismer, S. *Introduction to Coevolutionary Theory* (W. H. Freeman, 2017).
45. Birskis-Barros, I., Freitas, A. V. L. & Guimarães, P. R. Jr. Habitat generalist species constrain the diversity of mimicry rings in heterogeneous habitats. *Sci. Rep.* **11**, 5072 (2021).
46. Bezanson, J., Edelman, A., Karpinski, S. & Shah, V. B. Julia: a fresh approach to numerical computing. *SIAM Rev.* **59**, 65–98 (2017).
47. R Core Team. *R: A Language and Environment for Statistical Computing*. <https://www.R-project.org/> (R Foundation for Statistical Computing, 2022).
48. Cosmo, L. G. Indirect effects shape species fitness in coevolved mutualistic networks (version 1.0.0). <https://doi.org/10.5281/zenodo.7945239> (2023).

Acknowledgements This study was financed in part by the Coordenação de Aperfeiçoamento de Pessoal de Nível Superior – Brasil (CAPES), finance code 001. L.G.C. is funded by a São Paulo Research Foundation PhD scholarship (FAPESP; grants 2019/22146-3 and 2022/07939-0). P.R.G. is funded by Brazil's Council for Scientific and Technological Development (CNPq; grant 307134/2017-2), FAPESP (grant 2018/14809-0) and the Royal Society (CHL/R1/180156). A.P.A.A. was supported by CAPES, finance code 001, and FAPESP (grant 2016/14277-2). M.M.P. is funded by FAPESP (grant 2019/25478-7) and CNPq (grant 313059/2022-5). M.A.M.A. is funded by FAPESP (grant 2021/14335-0-ICTP-SAIFR), and by CNPq (grant 301082/2019-7). A.V. is supported by the Spanish Ministry of Science, Innovation, and Universities (PGC2018-099772-B-I00). P.J. is funded by the Spanish Ministry of Science, Innovation, and Universities

(CGL2017-82847-P), LifeWatch ERIC-SUMHAL (LIFEWATCH-2019-09-CSIC-13)/FEDER-EU funding), and the VI and VII Research Funding Program from the Universidad de Sevilla (2021/00000826). J.B. is supported by the Swiss National Science Foundation (grant 310030_197201). We thank R. Cogni, M. A. R. Mello, C. R. Montoya and M. C. Vidal for comments on previous versions of this manuscript.

Author contributions All authors designed the study. L.G.C., P.R.G. and M.A.M.A. derived the fitness function. L.G.C. and P.R.G. developed the analytical approximations. L.G.C. performed simulations and conducted analyses. A.V. and P.J. contributed to data acquisition and analysis of the field experiment. L.G.C., P.R.G. and J.B. wrote the first draft of the manuscript, and all authors contributed substantially to the final draft.

Competing interests The authors declare that they have no competing financial interests.

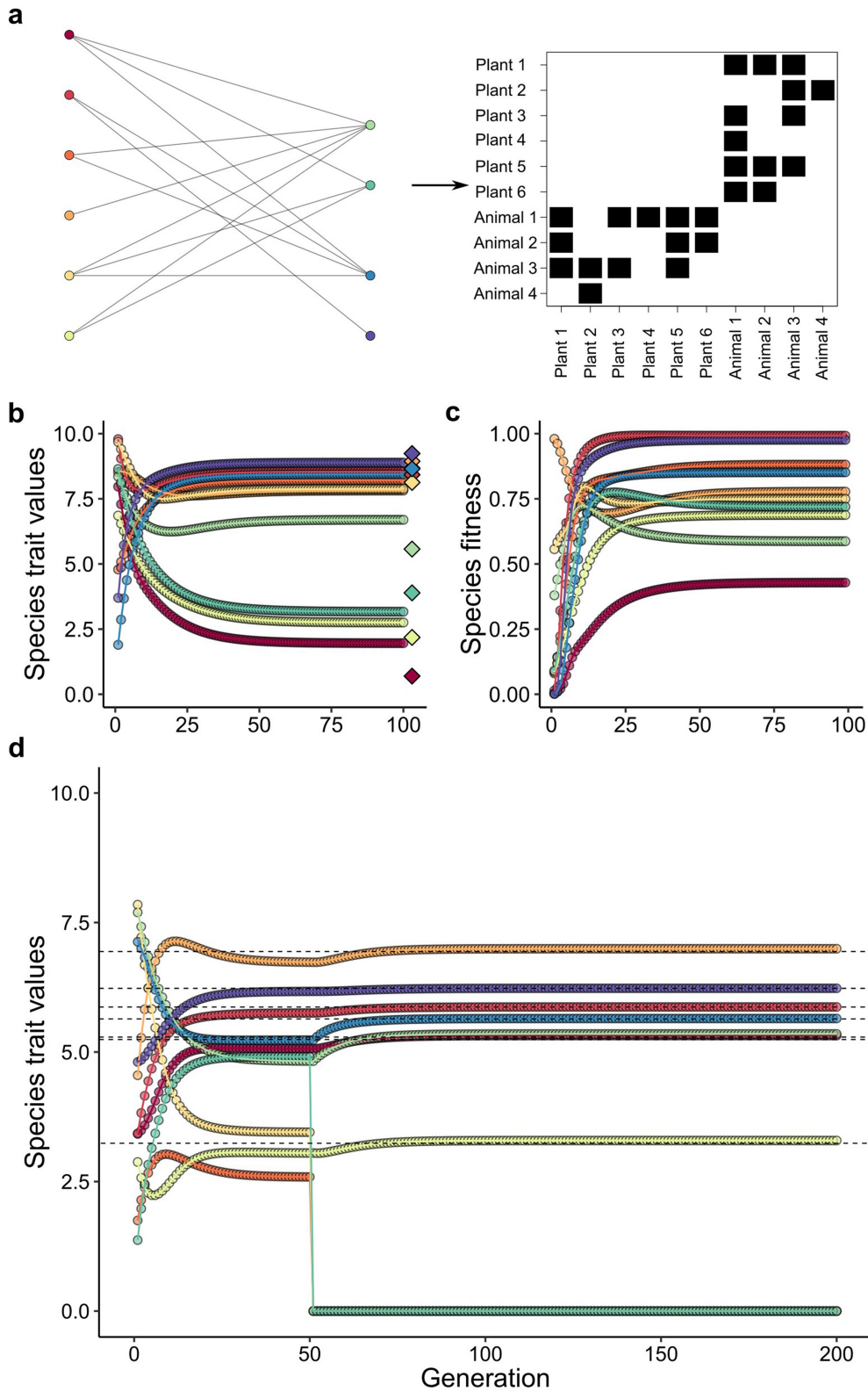
Additional information

Supplementary information The online version contains supplementary material available at <https://doi.org/10.1038/s41586-023-06319-7>.

Correspondence and requests for materials should be addressed to Leandro G. Cosmo.

Peer review information *Nature* thanks Thilo Gross and the other, anonymous, reviewer(s) for their contribution to the peer review of this work.

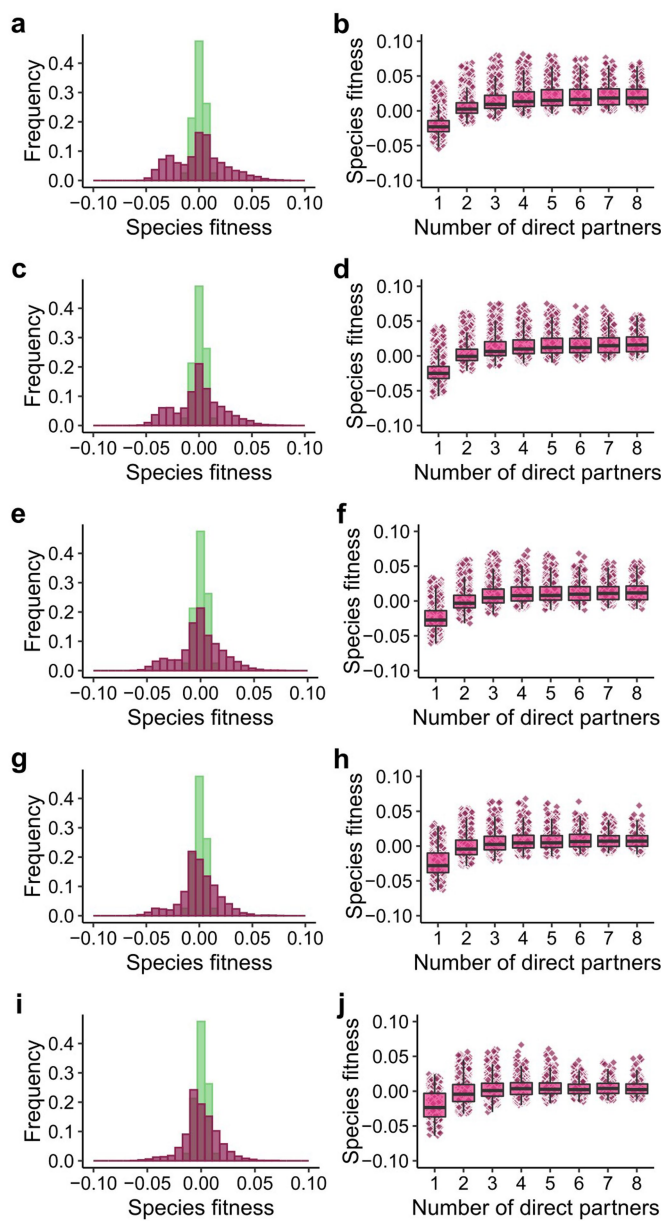
Reprints and permissions information is available at <http://www.nature.com/reprints>.



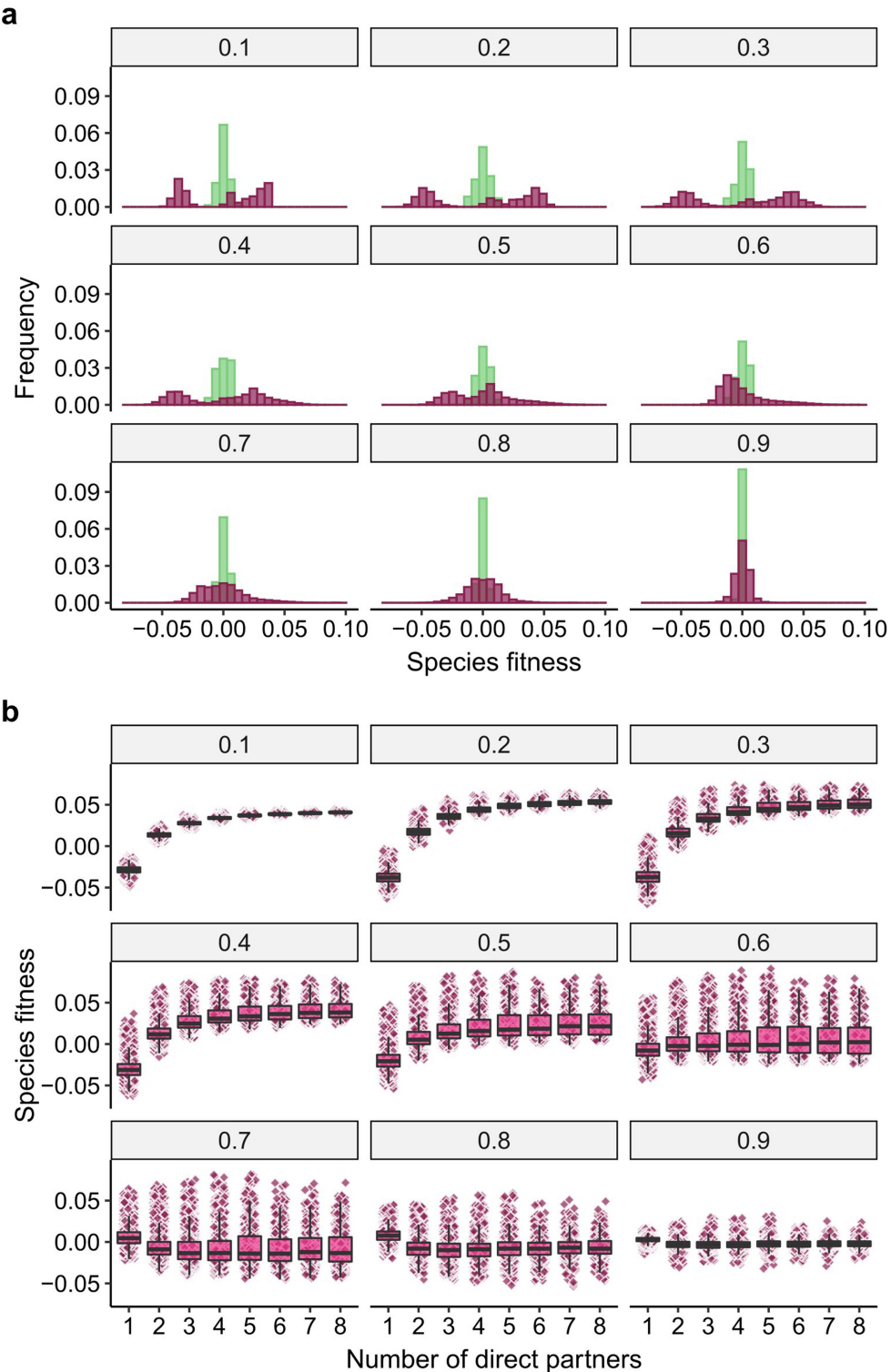
Extended Data Fig. 1 | Species traits and fitness quickly reach equilibrium values after coevolving in mutualistic networks. **a–c**, Example for an ant-plant mutualistic network (panel **a**) of how species traits (panel **b**) and fitness (panel **c**) quickly reach a coevolutionary equilibrium. **d**, The coevolutionary equilibrium is reached even if not all species survive throughout the dynamics, as illustrated by three species that were randomly extinct from the network (for illustrative purposes, species whose trait values reach zero). Each point and line correspond

to the values for each species in the network (represented by different colors). The diamond-shaped points on the right of panel **b** represent the environmental optima of each species (θ_i). The dashed lines in panel **d** represent the trait values at equilibrium predicted by equation (12) using the matrix of the interactions among surviving species. Parameter values are as follows: $\sigma_{Gz_i}^2 = 1.0$, $q_i = 0.2$, $\alpha = 0.2$, $m_i = 0.5$. Initial trait values and environmental optima were sampled from a uniform distribution $U[0, 10]$.

Article

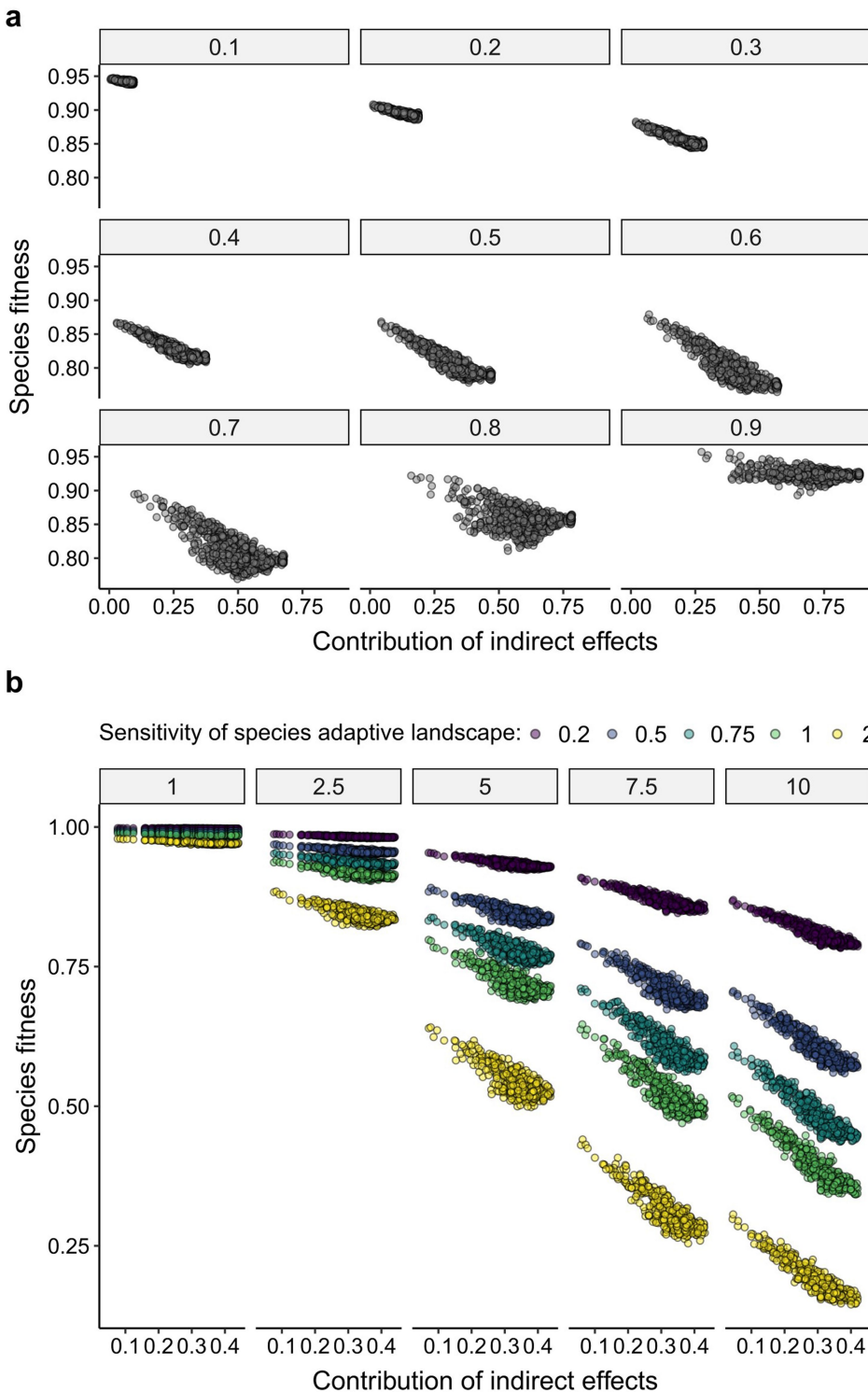


Extended Data Fig. 2 | Coevolution in mutualistic networks increases the variability in species fitness when a certain percentage of the species with the lowest fitness become extinct, and the surviving species coevolve to a new equilibrium. Each set of panels represents a specific scenario where a certain percentage of the species in the network experience extinction after reaching the initial coevolutionary equilibrium. In all scenarios extinctions occurred in a specific order, starting with the species possessing the lowest fitness until a desired percentage of extinctions was reached. The corresponding extinction percentages for each scenario are as follows: **a–b**, 10%; **c–d**, 20%; **e–f**, 30%; **g–h**, 40%; and **i–j**, 50%. In all panels the red histogram bars depict the distribution of fitness of the surviving species in the new coevolutionary equilibrium for 10^3 numerical simulations parameterized with the initial structure of empirical networks ($n = 186$ empirical networks). Green histogram bars correspond to the scenario in which species coevolve as isolated pairs and there are no extinctions. In the boxplots each point corresponds to the mean value for 10^3 numerical simulations for a given species coevolving in the empirical mutualistic networks ($n = 186$ empirical networks). Fitness values are rescaled relative to the average of the scenario in which species coevolve in networks or as isolated pairs. Other parameter values are as follows: $\sigma_{G_i}^2 = 1.0$, $\phi_i = 0.2$, $\alpha = 0.2$, and $m_i = 0.5$. θ_i and initial trait values were sampled from a uniform distribution $U[0, 10]$.



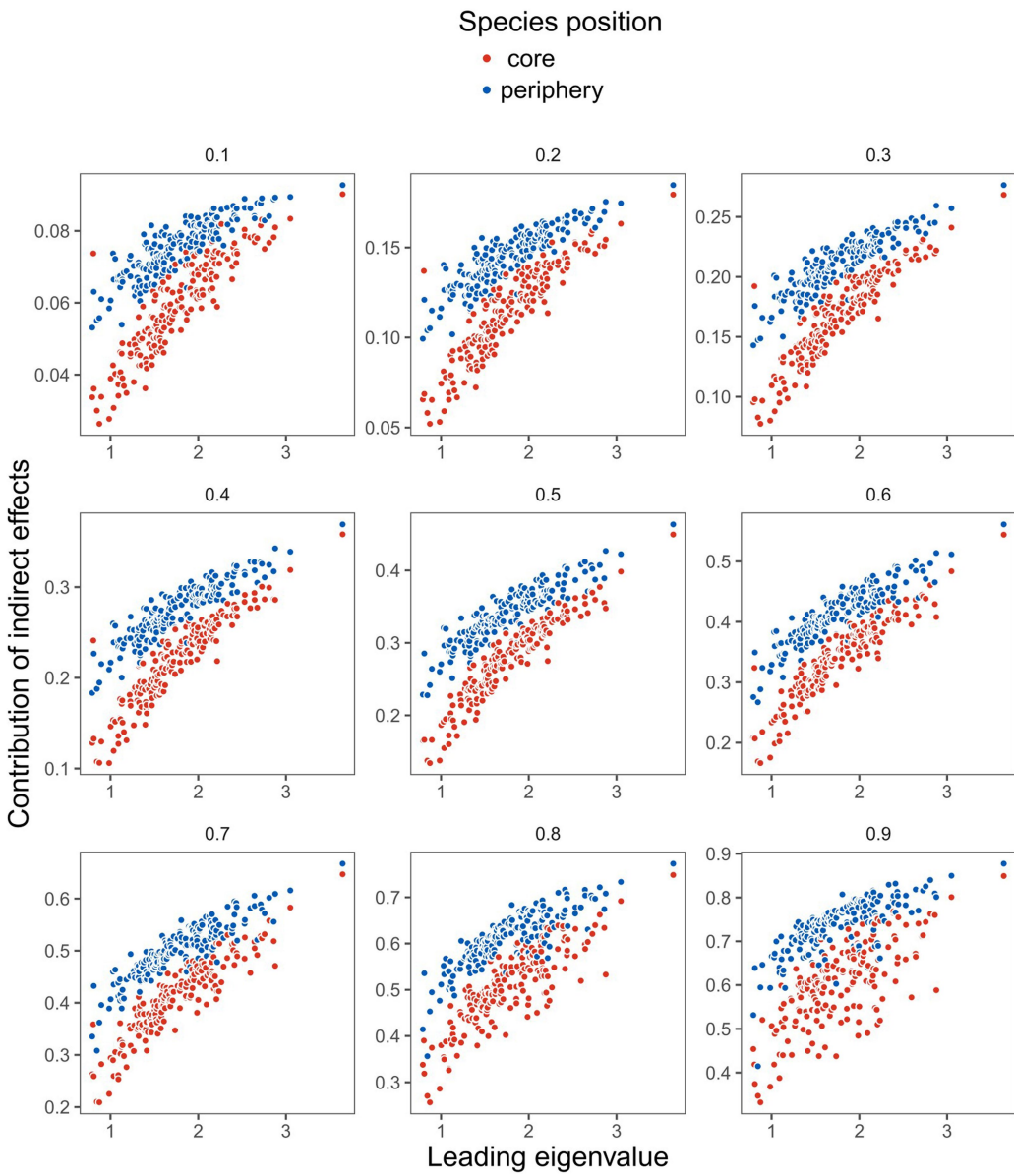
Extended Data Fig. 3 | Coevolution in mutualistic networks increases the variability in species fitness for different levels of strength of mutualistic selection. **a.**, Histogram showing the distribution of mean equilibrium fitness of species for 10^3 numerical simulations of a pair of coevolving species (green histogram bars), or of species within the 186 empirical networks used to parameterize the model (red histogram bars), for different values of m_i (values above each panel). **b.**, Boxplot showing how species fitness vary with

the number of mutualistic partners for different values of m_i (the intensity of mutualistic selection, values above each panel). Each point corresponds to the mean value for 10^3 numerical simulations for a given species. In all panels fitness values are rescaled relative to the average of each scenario and m_i (coevolution in pairs or in networks). Other parameter values are as follows: $\sigma_{Gz_i}^2 = 1.0$, $q_i = 0.2$, $\alpha = 0.2$, and m_i as indicated on top of each panel. θ_i and initial trait values were sampled from a uniform distribution $U[0, 10]$.



Extended Data Fig. 4 | Indirect effects drive species fitness for different parameterizations of the model. **a**, Examples of how indirect evolutionary effects drive the fitness of species in numerical simulations across all empirical networks ($n=186$ empirical networks) for different values of m_i (values above each panel), for species with five mutualistic partners. **b**, Examples of how indirect evolutionary effects drive the fitness of species in numerical simulations across all empirical networks ($n=186$ empirical networks) for different intervals of θ_i (values above each panel), and sensitivity of species

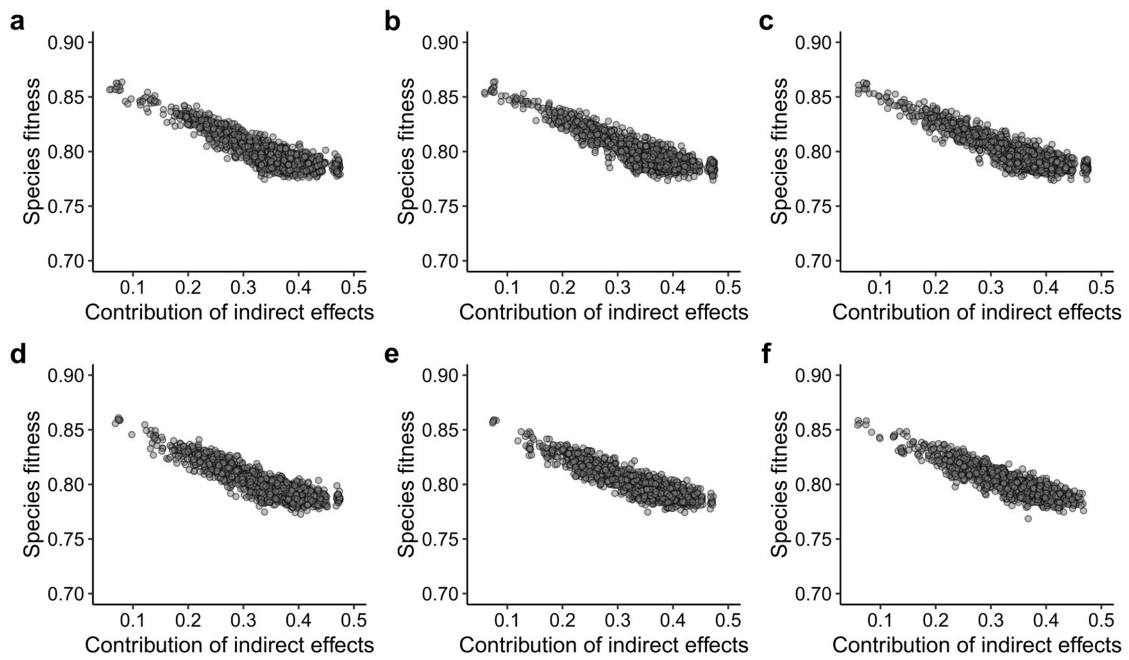
adaptive landscapes (q_i , different colors) for species with five mutualistic partners. Points in all panels represent average results for 10^3 numerical simulations of each combination of empirical network and parameter values. Other parameter values are as follows: $\sigma_{G_i}^2 = 1.0$ and $\alpha = 0.2$. Values of m_i and q_i as indicated on each panel. In **a**, θ_i and initial trait values were sampled from a uniform distribution $U[0, 10]$, while in **b** the upper bound of the uniform distribution is indicated in the values above each panel.



Extended Data Fig. 5 | Peripheral species are more affected by indirect effects drive for different networks and levels of mutualistic selection.

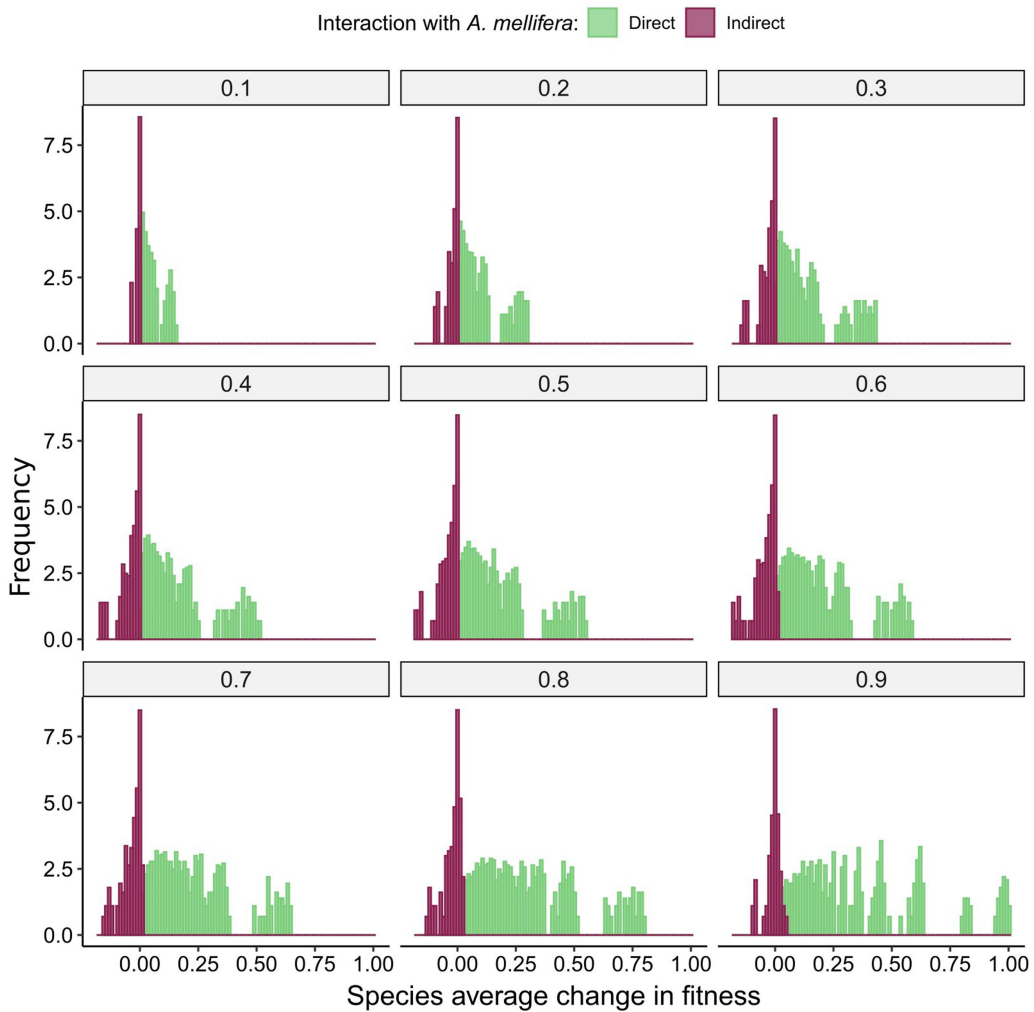
Results from numerical simulations parameterized with the structure of empirical networks ($n=186$ empirical networks), showing how the contribution of indirect evolutionary effects is smaller for core than peripheral species within the same network. This result holds for all values of m_i , the intensity of mutualistic selection (values above each panel). Each point corresponds to

the average for 10^3 numerical simulations for each combination of species position (core or peripheral), empirical network and m_i . Points of different colors correspond to species that were classified either as core species (red points) or peripheral species (blue points). Parameter values are as follows: $m_i = \text{variable}$, $\sigma_{Gz_i}^2 = 1.0$, $\alpha_i = 0.2$, θ_i and initial trait values were sampled from a uniform statistical distribution $U[0, 10]$.



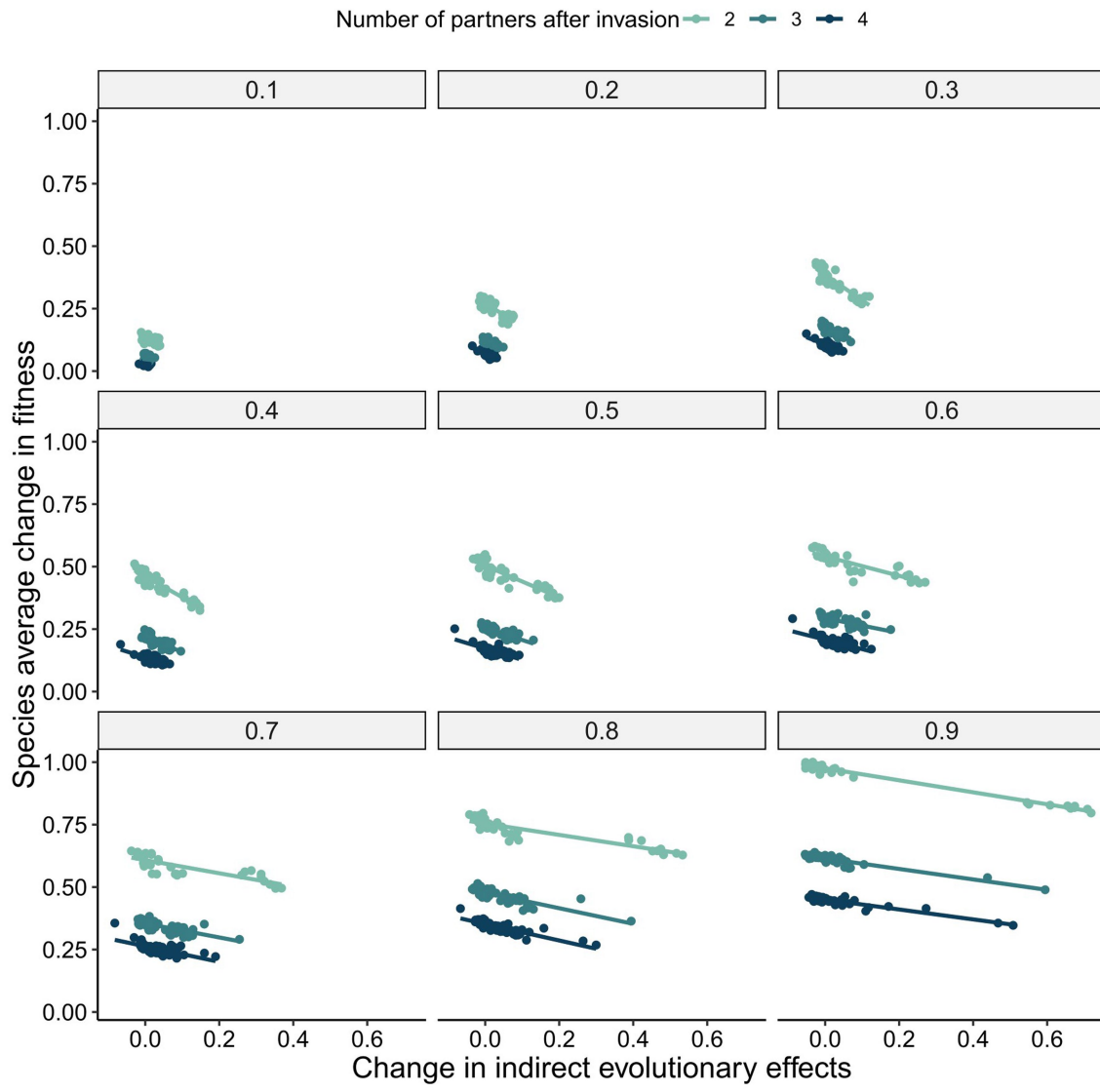
Extended Data Fig. 6 | Indirect effects drive the fitness of surviving species when the least fit species become extinct, and the surviving ones coevolve to a new equilibrium. Each panel corresponds to scenarios in which a certain percentage of the species in the network underwent extinction after reaching a first coevolutionary equilibrium. For all scenarios extinctions occurred in a specific order, starting with the species possessing the lowest fitness, until a given percentage of extinctions was reached. The corresponding percentage of species extinct are as follows: **a**, scenario without extinctions; **b**, 10%; **c**, 20%;

d, 30%; **e**, 40%; and **f**, 50%. Points in each panel represent average results for species with three mutualistic partners across 10^3 numerical simulations parameterized with the initial structure of 186 empirical networks. In panels **b-f**, indirect evolutionary effects were computed from the matrix of evolutionary effects (\mathbf{Q} -matrix) among the surviving species (equation 14). Parameter values are as follows: $m_i = 0.5$, $\sigma_{Gz_i}^2 = 1.0$, $q_i = 0.2$, $\alpha = 0.2$. θ_i and initial trait values were sampled from a uniform statistical distribution $U[0, 10]$.



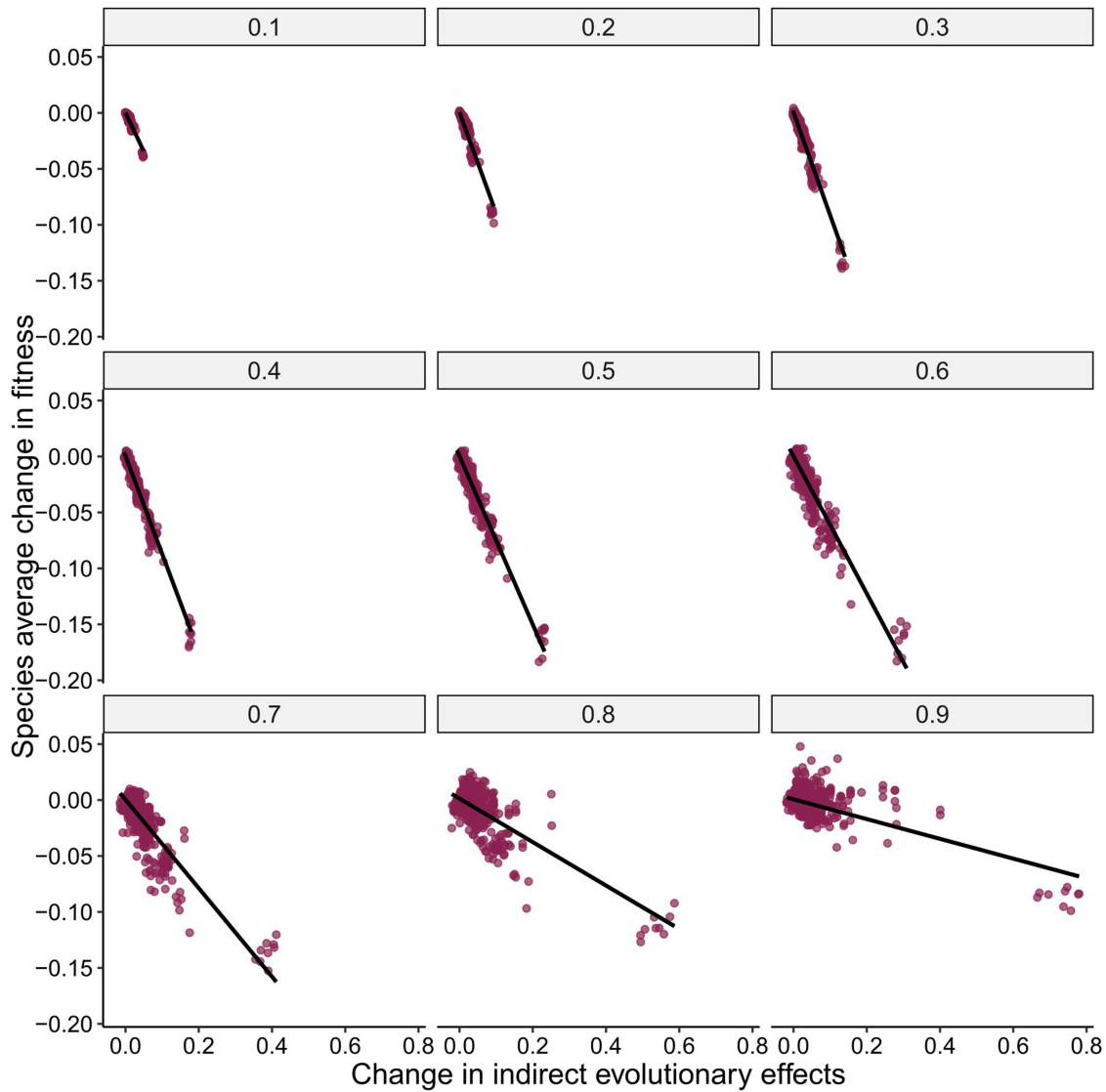
Extended Data Fig. 7 | Invasion of a network by a supergeneralist changes the fitness of native species via coevolution for different levels of mutualistic selection. Histograms showing the average change in native species fitness ($n=10^3$ numerical simulations for each of the 73 empirical networks) after coevolving with the invasive species for different values of m_i

(the intensity of mutualistic selection, values above each panel). The frequency in the y-axis represents $\log(\text{Counts})$. Other parameter values are as follows: $\sigma_{Gz_i}^2 = 1.0$, $q_i = 0.2$, $\alpha = 0.2$, and m_i as indicated on top of each panel. θ_i and initial trait values were sampled from a uniform distribution $U[0, 10]$.



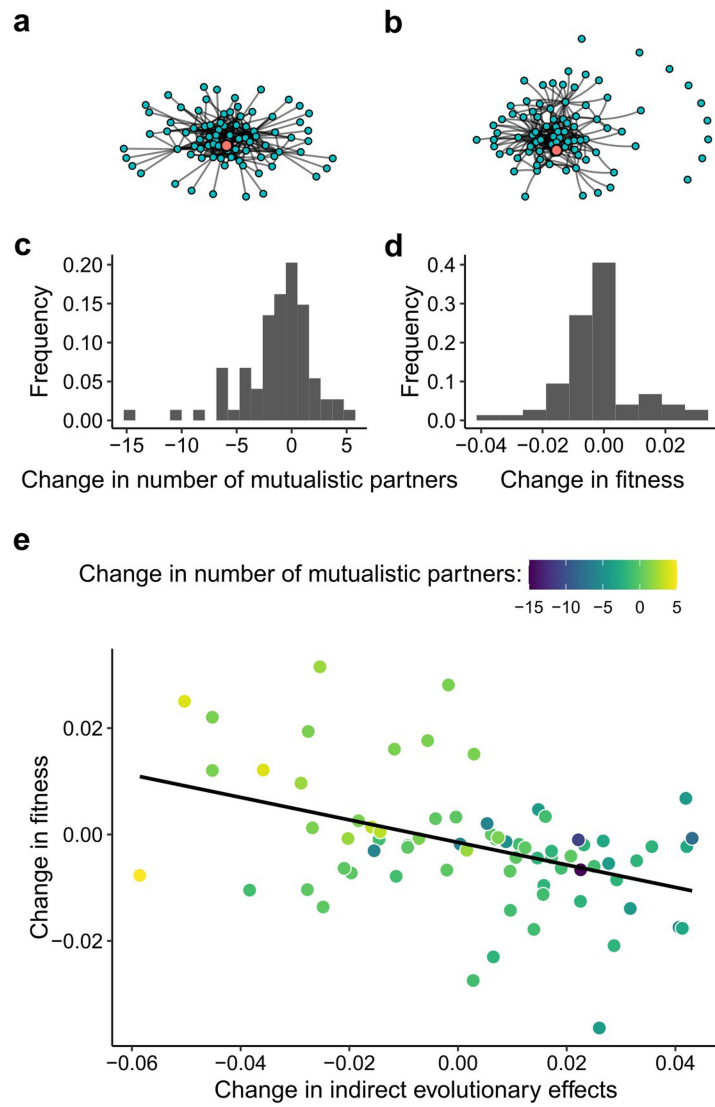
Extended Data Fig. 8 | Direct and indirect evolutionary effects drive the change in fitness of native species directly interacting with a supergeneralist invader. Relationship between the average change in species fitness ($n = 10^3$ numerical simulations for each of the 73 empirical networks) after the invasion and the change in the contribution of indirect evolutionary effects for direct

partners of *A. mellifera* and for different values of m_i (the intensity of mutualistic selection, values above each panel). Parameter values are as follows: $\sigma_{Gz_i}^2 = 1.0$, $q_i = 0.2$, $\alpha = 0.2$, and m_i as indicated on top of each panel. θ_i and initial trait values were sampled from a uniform distribution $U[0, 10]$.



Extended Data Fig. 9 | Indirect evolutionary effects drive the change in fitness of native species only indirectly interacting with a supergeneralist invader. Relationship between the average change in species fitness ($n = 10^3$ numerical simulations for each of the 73 empirical networks) after the invasion and the change in the contribution of indirect evolutionary effects for indirect

partners of *A. mellifera* and for different values of m_i (the intensity of mutualistic selection, values above each panel). Other parameter values are as follows: $\sigma_{Gz}^2 = 1.0$, $q_i = 0.2$, $\alpha = 0.2$, and m_i as indicated on top of each panel. θ_i and initial trait values were sampled from a uniform distribution $U[0, 10]$.



Extended Data Fig. 10 | Indirect evolutionary effects and rewiring of interactions shape the fitness consequences of the invasion of a network by the supergeneralist *A. mellifera*. **a–b**, Representations of the (a) pre- (before beekeeping activity) and (b) post-*Apis* (after beekeeping activity) network structures, showing how the invasion by *A. mellifera* (in red) reorganizes interactions. **c–d**, Histograms showing (c) the change in the number of partners and (d) the change in fitness that native species experienced after coevolving

with *A. mellifera*. **e**, Relationship between the change in indirect evolutionary effects caused by *A. mellifera* and the change in the fitness of native species. The results in panels **d** and **e** correspond to the average results for the native species of 10^3 numerical simulations of the coevolutionary dynamics in the pre- and post-*Apis* networks. Parameter values are as follows: $m_i = 0.5$, $\sigma_{Gz_i}^2 = 1.0$, $q_i = 0.2$, $\alpha = 0.2$. θ_i and initial trait values were sampled from a uniform statistical distribution $U[0, 10]$.

Reporting Summary

Nature Portfolio wishes to improve the reproducibility of the work that we publish. This form provides structure for consistency and transparency in reporting. For further information on Nature Portfolio policies, see our [Editorial Policies](#) and the [Editorial Policy Checklist](#).

Statistics

For all statistical analyses, confirm that the following items are present in the figure legend, table legend, main text, or Methods section.

n/a Confirmed

- The exact sample size (n) for each experimental group/condition, given as a discrete number and unit of measurement
- A statement on whether measurements were taken from distinct samples or whether the same sample was measured repeatedly
- The statistical test(s) used AND whether they are one- or two-sided
Only common tests should be described solely by name; describe more complex techniques in the Methods section.
- A description of all covariates tested
- A description of any assumptions or corrections, such as tests of normality and adjustment for multiple comparisons
- A full description of the statistical parameters including central tendency (e.g. means) or other basic estimates (e.g. regression coefficient) AND variation (e.g. standard deviation) or associated estimates of uncertainty (e.g. confidence intervals)
- For null hypothesis testing, the test statistic (e.g. F , t , r) with confidence intervals, effect sizes, degrees of freedom and P value noted
Give P values as exact values whenever suitable.
- For Bayesian analysis, information on the choice of priors and Markov chain Monte Carlo settings
- For hierarchical and complex designs, identification of the appropriate level for tests and full reporting of outcomes
- Estimates of effect sizes (e.g. Cohen's d , Pearson's r), indicating how they were calculated

Our web collection on [statistics for biologists](#) contains articles on many of the points above.

Software and code

Policy information about [availability of computer code](#)

Data collection	All of the empirical networks used to parameterize our numerical simulations are available at the Web of Life database (www.web-of-life.es).
Data analysis	Numerical simulations were conducted in the Julia programming language (v1.5.0), while analysis of the numerical simulations were conducted using the R programming language (V4.0.0). All the code to perform the numerical simulations used in this study is available in a GitHub repository (https://github.com/lcosmo/Cosmo_et_el_indirect_effects_fitness) and in Zenodo (doi:10.5281/zenodo.7945239).

For manuscripts utilizing custom algorithms or software that are central to the research but not yet described in published literature, software must be made available to editors and reviewers. We strongly encourage code deposition in a community repository (e.g. GitHub). See the Nature Portfolio [guidelines for submitting code & software](#) for further information.

Data

Policy information about [availability of data](#)

All manuscripts must include a [data availability statement](#). This statement should provide the following information, where applicable:

- Accession codes, unique identifiers, or web links for publicly available datasets
- A description of any restrictions on data availability
- For clinical datasets or third party data, please ensure that the statement adheres to our [policy](#)

The dataset of empirical networks used in this study is available in a GitHub repository (https://github.com/lcosmo/Cosmo_et_el_indirect_effects_fitness), in Zenodo (doi:10.5281/zenodo.7945239), and in the Web-of-Life Database (www.web-of-life.es).

Human research participants

Policy information about [studies involving human research participants and Sex and Gender in Research](#).

Reporting on sex and gender	<input type="checkbox"/> This information has not been collected.
Population characteristics	<input type="checkbox"/> See above.
Recruitment	<input type="checkbox"/> See above.
Ethics oversight	<input type="checkbox"/> See above.

Note that full information on the approval of the study protocol must also be provided in the manuscript.

Field-specific reporting

Please select the one below that is the best fit for your research. If you are not sure, read the appropriate sections before making your selection.

Life sciences Behavioural & social sciences Ecological, evolutionary & environmental sciences

For a reference copy of the document with all sections, see nature.com/documents/nr-reporting-summary-flat.pdf

Ecological, evolutionary & environmental sciences study design

All studies must disclose on these points even when the disclosure is negative.

Study description	In our study we combined analytical approximations and numerical simulations of a coevolutionary model to understand how indirect evolutionary effects drive species fitness in mutualistic networks.
Research sample	We parameterized our model with the structure of 186 empirical mutualistic networks.
Sampling strategy	We used all of the available empirical networks in the Web of Life database.
Data collection	All of the empirical networks were obtained from the Web of Life database (www.web-of-life.es).
Timing and spatial scale	This is not applicable to our study since its a theoretical study that does not involve field work.
Data exclusions	No data were excluded from the analysis.
Reproducibility	All of the code, as well as the empirical datasets used to parameterize our analysis are available, allowing reliable reproduction of all of our results.
Randomization	This is not applicable to our study since its a theoretical study that does not involve field work.
Blinding	This is not applicable to our study since its a theoretical study that does not involve field work.

Did the study involve field work? Yes No

Reporting for specific materials, systems and methods

We require information from authors about some types of materials, experimental systems and methods used in many studies. Here, indicate whether each material, system or method listed is relevant to your study. If you are not sure if a list item applies to your research, read the appropriate section before selecting a response.

Materials & experimental systems

n/a	Involved in the study
<input checked="" type="checkbox"/>	Antibodies
<input checked="" type="checkbox"/>	Eukaryotic cell lines
<input checked="" type="checkbox"/>	Palaeontology and archaeology
<input checked="" type="checkbox"/>	Animals and other organisms
<input checked="" type="checkbox"/>	Clinical data
<input checked="" type="checkbox"/>	Dual use research of concern

Methods

n/a	Involved in the study
<input checked="" type="checkbox"/>	ChIP-seq
<input checked="" type="checkbox"/>	Flow cytometry
<input checked="" type="checkbox"/>	MRI-based neuroimaging